ISSN 1063-7796, Physics of Particles and Nuclei, 2020, Vol. 51, No. 3, pp. 301–304. © Pleiades Publishing, Ltd., 2020.

Anisotropic Flow Measurements from the NA61/SHINE and NA49 Beam Momentum Scan Programs at CERN SPS

E. Kashirin[a, d, *], I. Selyuzhenkov[a, b, **], O. Golosov[a], and V. Klochkov[b, c]
(for the NA49 and NA61/SHINE Collaborations)

[a] *National Research Nuclear University MEPhI (Moscow Engineering Physics Institute), Moscow, Russia*
[b] *GSI Helmholtzzentrum für Schwerionenforschung, Darmstadt, Germany*
[c] *Goethe-University Frankfurt, Frankfurt, Germany*
[d] *Institute for Nuclear Research RAS, Moscow, Russia*
**e-mail: evgeny.kashirin@cern.ch*
***e-mail: ilya.selyuzhenkov@gmail.com*

Received September 20, 2019; revised October 28, 2019; accepted November 20, 2019

Abstract—The NA61/SHINE experiment at the CERN SPS has recently extended its program for the energy scan with Pb ions. In the past, the NA49 experiment, which preceded the NA61/SHINE, has also recorded data for Pb–Pb collisions at different energies. Together, the two experiments cover wide range of collision energies in the beam momentum range of 13–150A GeV/c provided by CERN SPS, which has a significant overlap with the ongoing second phase of the beam energy scan program (BES-II) at RHIC. The directed and elliptic flow relative to the projectile spectator plane are measured with the new NA61/SHINE data for Pb–Pb collisions at 13 and 30A GeV/c and revised existing NA49 data at 40A GeV. New results extend the existing world data available from the previous NA49 measurements and ongoing BES-II and fixed-target programs at STAR. The developed analysis techniques are also relevant for measurements at the future CBM experiment at FAIR and the MPD experiment at NICA.

DOI: 10.1134/S1063779620030144

INTRODUCTION

Spatial asymmetry of initial energy density in the overlap region of the colliding relativistic nuclei is converted via interaction between produced particles to the asymmetry of momentum distribution of particles in the final state. The resulting asymmetry encodes important information about the transport properties of the QCD matter created during the collision. Asymmetry is usually quantified with the coefficients v_n in a Fourier decomposition of the azimuthal distribution of produced particles relative to the reaction plane spanned by the impact parameter and the beam direction [1]:

$$\rho(\varphi - \Psi_{\mathrm{RP}}) = \frac{1}{2\pi}\left(1 + 2\sum_{n=1}^{\infty} v_n \cos[n(\varphi - \Psi_{\mathrm{RP}})]\right). \quad (1)$$

The energy dependency of flow coefficients is of particular importance. At the SPS energies it is expected that the slope of proton directed flow at midrapidity, dv_1/dy, changes its sign [2]. The Elliptic flow, v_2, also turns from out-of-plane to in-plane at the collision energies of several GeV [3].

Fixed-target configuration of the NA49 and NA61/SHINE experiments allow to perform measurements up to the forward rapidity where the projectile spectators appear. The reaction plane angle Ψ_{RP} is estimated using the transverse energy distribution of projectile spectators which is measured by forward calorimeters.

DATA SAMPLE AND ANALYSIS CONFIGURATION

The NA49 experiment operated in 1994–2000 [4]. Tracking system of NA49 consisted of four big time-projection chambers (TPCs). Two vertex TPCs (VTPC1 and VTPC2) were put into magnetic field to measure 3D momentum of charged particles. Another two (MTPC Left/Right) were placed outside the magnetic field to additionally perform precise dE/dx measurements necessary for particle identification. Tracking system covered forward hemisphere and allowed to identify charged particles down to zero p_T. The Veto calorimeter (VCAL) was installed 20 meters downstream the target behind the collimator and has a 2×2 transverse module granularity. The opening of the collimator was adjusted such that beam particles, projectile fragments and spectator neutrons and protons can reach the calorimeter. Ring (RCAL) calorim-

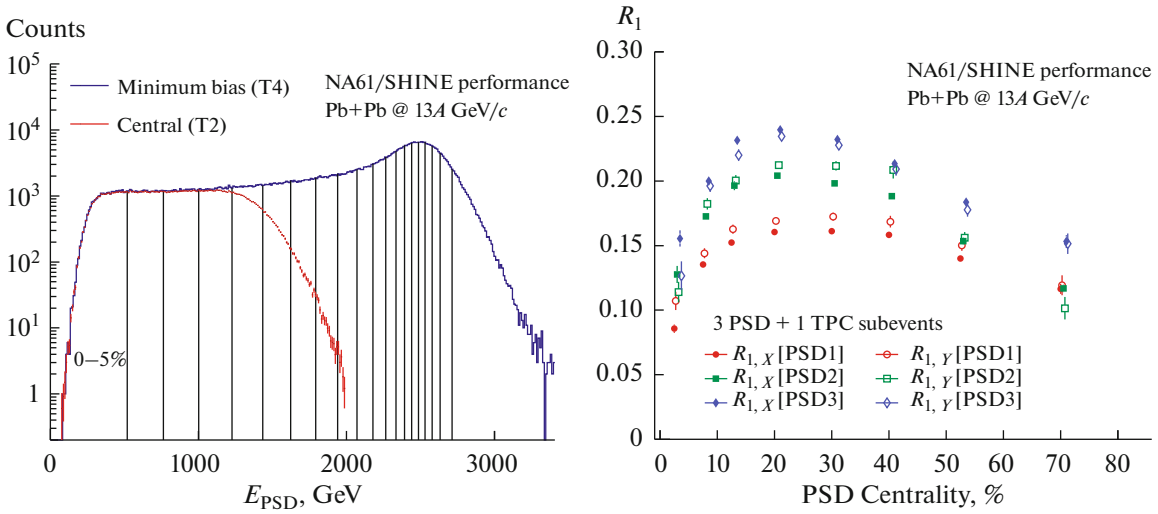

Fig. 1. Left: PSD energy distribution for central (T2) and minimum bias (T4) triggers. Dashed vertical lines mark the borders of event (centrality) classes. Right: Resolution correction factors $R^{A}_{1,\alpha}$ are obtained for PSD subevents using the 3 + 1-subevent method.

eter was positioned at 18 m from the target in front of collimator and it had transverse granularity of 10 rings with 24 modules each.

The NA61/SHINE facility is the successor of NA49 experiment [5]. It's central part is formed by the four upgraded TPCs. The RCAL and VCAL were replaced with the Projectile Spectator Detector (PSD).

Analysis details of the NA49 experiment are described in [6] and of the NA61/SHINE data for Pb–Pb collisions at 30A GeV/c in [7]. For 40A GeV data 340k (440k) minimal bias (central) events were selected. Below we describe only details of the analysis of the Pb + Pb collisions at 13A GeV/c recorded by NA61/SHINE in 2016.

Events with fitted vertex position close to the target region were selected. Events overlapping in time (pileup) were rejected. After event selection, the available statistics is 580k events for the minimum bias trigger (T4) and 480k events for the central trigger (T2) which was fully efficient in the 0–15% centrality class. Charged particle tracks with total number of clusters in the TPCs larger than 30 and number of clusters in the vertex TPCs larger than 15 were accepted for flow analysis. To avoid track splitting, the number of hits associated to the track was required to be more than 55% of the maximum number of points along the particle trajectory. Primary tracks were selected based on the distance of closest approach to the primary vertex in the plane transverse to the beam direction, which was required to be less than 2 cm in x direction and less than 1 cm in y direction. Charged pion and proton identification was based on specific energy loss dE/dx in the TPCs.

The PSD is sensitive mostly to spectator fragments (outer modules are also sensitive to produced particles) and is used for event (centrality) classification and reaction plane determination. Event classification is performed following the procedure described in [8]. Figure 1 (left) shows the result of the event classification procedure using the energy measured at forward rapidity with the PSD.

ANALYSIS TECHNIQUE

Flow coefficients v_n were measured using scalar-product method [9] from correlations of two-dimensional flow vectors $\mathbf{q_n}$ and $\mathbf{Q_n}$. The $\mathbf{q_n}$ is calculated event-by-event from azimuthal angles φ_i of the ith particle's momentum:

$$\mathbf{q_n} = \frac{1}{M}\sum_{i=1}^{M} \mathbf{u}_{1,\mathbf{n}}, \tag{2}$$

where $\mathbf{u_{n,i}} = (\cos n\phi_i, \sin n\phi_i)$ and M is selected particle' multiplicity in a given p_T and rapidity range. Spectators' symmetry plane is estimated with the $\mathbf{Q}_1$ direction determined from azimuthal asymmetry of energy deposition in PSD subevent A:

$$\mathbf{Q}_1^{\mathrm{A}} = \frac{1}{E_{\mathrm{A}}}\sum_{i=1}^{N_A} E_i \mathbf{n_i}, \tag{3}$$

where $E_{\mathrm{A}} = \sum_{i=1}^{N_A} E_i$ is the total energy deposited to PSD subevent A. Unit vector $\mathbf{n_i}$ points in the direction of the center of ith PSD module and E_i is its measured energy.

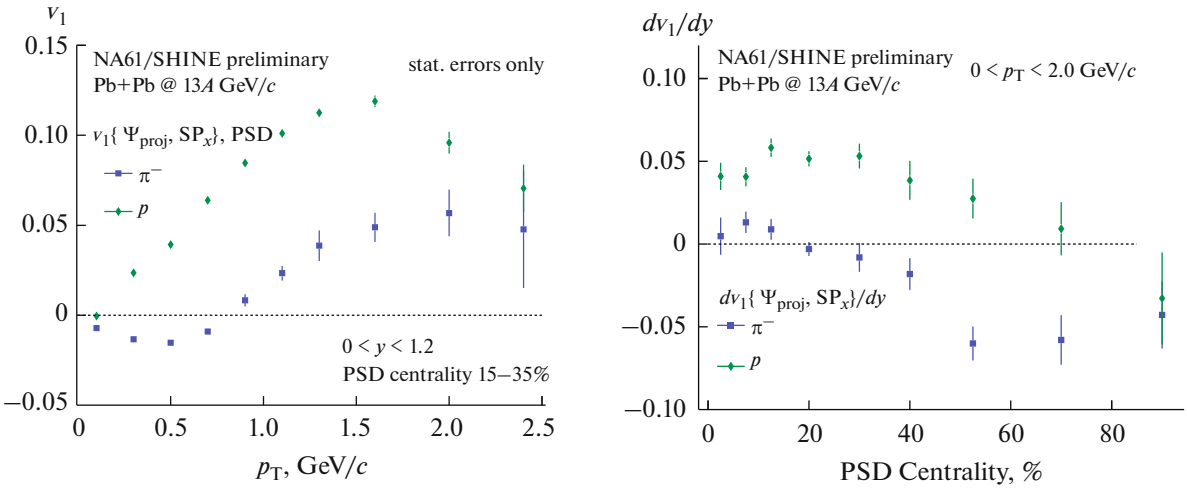

Fig. 2. Left: negatively charged pion and proton directed flow $v_1(p_T)$ for 15–35% centrality class. Right: slope of directed flow dv_1/dy at $y = y_{CM}$ as function of the collision centrality.

Independent estimates of directed flow v_1 an elliptic flow v_2 are given by equations

$$v_1^{\alpha}\{A\} = \frac{2\left\langle q_{1,\alpha}Q_{1,\alpha}^{A}\right\rangle}{R_{1,\alpha}^{A}},$$
$$v_2^{\alpha\beta\gamma}\{A,B\} = \kappa_{\alpha\beta\gamma}\frac{4\left\langle q_{2,\alpha}Q_{1,\beta}^{A}Q_{1,\gamma}^{B}\right\rangle}{R_{1,\beta}^{A}R_{1,\gamma}^{B}}, \quad (4)$$

where $\alpha,\beta,\gamma = x, y$ are q_1 and Q_1 components and A, B—PSD subevents. Only four combinations of $\alpha\beta\gamma$ are possible. Coefficient $\kappa_{\alpha\beta\gamma} = 1$ for $\alpha\beta\gamma = xxx$, yxy and yyx, $\kappa_{\alpha\beta\gamma} = -1$ for $\alpha\beta\gamma = xyy$.

The previous analyses of 30A GeV/c and 40A GeV were based on a three PSD subevent method of estimating the resolution correction factor $R_{1,\alpha}^{A}$ [6, 7]. At lower collision energy the hadronic shower sharing between adjacent PSD subevents introduces considerable bias especially for central events. To avoid correlations from the shower in the neighbouring subevents we extended the method by introducing additional 4th (TPC) subevent to the correlation. The **Q**-vector for the TPC subevent was calculated from the identified protons in the forward rapidity region ($0.8 < y - y_{CM} < 1.2$). The resolution correction factors for 3 + 1 subevent were calculated as

$$R_{1,\alpha}^{PSD1,3} = \sqrt{2\frac{\left\langle Q_{1,\alpha}^{PSD1}Q_{1,\alpha}^{PSD3}\right\rangle\left\langle Q_{1,\alpha}^{PSD1,3}Q_{1,\alpha}^{TPC}\right\rangle}{\left\langle Q_{1,\alpha}^{PSD3,1}Q_{1,\alpha}^{TPC}\right\rangle}}, \quad (5)$$

$$R_{1,\alpha}^{PSD2} = \frac{\left\langle Q_{1,\alpha}^{PSD2}Q_{1,\alpha}^{TPC}\right\rangle}{R_{1,\alpha}^{TPC}},$$
$$R_{1,\alpha}^{TPC} = \sqrt{2\frac{\left\langle Q_{1,\alpha}^{PSD1}Q_{1,\alpha}^{TPC}\right\rangle\left\langle Q_{1,\alpha}^{PSD3}Q_{1,\alpha}^{TPC}\right\rangle}{\left\langle Q_{1,\alpha}^{PSD1}Q_{1,\alpha}^{PSD3}\right\rangle}}. \quad (6)$$

Centrality dependence of $R_{1,\alpha}^{A}$ is shown in Fig. 1 (right).

RESULTS

Results are presented for correlations between negatively charged pions and protons produced by strong interaction processes and their weak and electromagnetic decays (in the TPC acceptance [10]) and all hadrons at forward rapidity (in the PSD acceptance [11]). The results were corrected for detector azimuthal non-uniformity using the procedure described in [12] and implemented in the QnCorrections framework [13, 14]. No corrections for p_T and y tracking and particle identification (PID) efficiency were applied in present analysis. Independent estimates for v_1 and v_2 using different PSD subevents are found to be consistent within statistical uncertainties. v_1 and v_2 evaluated using x and y components differs at high p_T for positive particles, possibly due to deflection of spectator protons by the magnetic field. Only x-component was used for v_1 calculations and an average of the (y, x, y) and (y, y, x) correlations was used for v_2. The PSD subevents were combined to obtain the final result.

Figure 2 (left) shows results for negatively charged pion and proton v_1 as a function of p_T. The $v_1(p_T)$ approaches zero at $p_T \to 0$ and for negatively charged pions, depends on centrality, it changes sign at $p_T \approx 0.7$–1.3 GeV/c. The slope of directed flow, dv_1/dy, is shown in Fig. 2 (right). It was calculated by fitting $v_1(y)$ for $|y| < 0.4$ with linear function. For both protons and negative pions it starts with positive values for central collisions and turns to negative values at certain centrality. This observation is consistent with recent STAR results from the BES data [2].

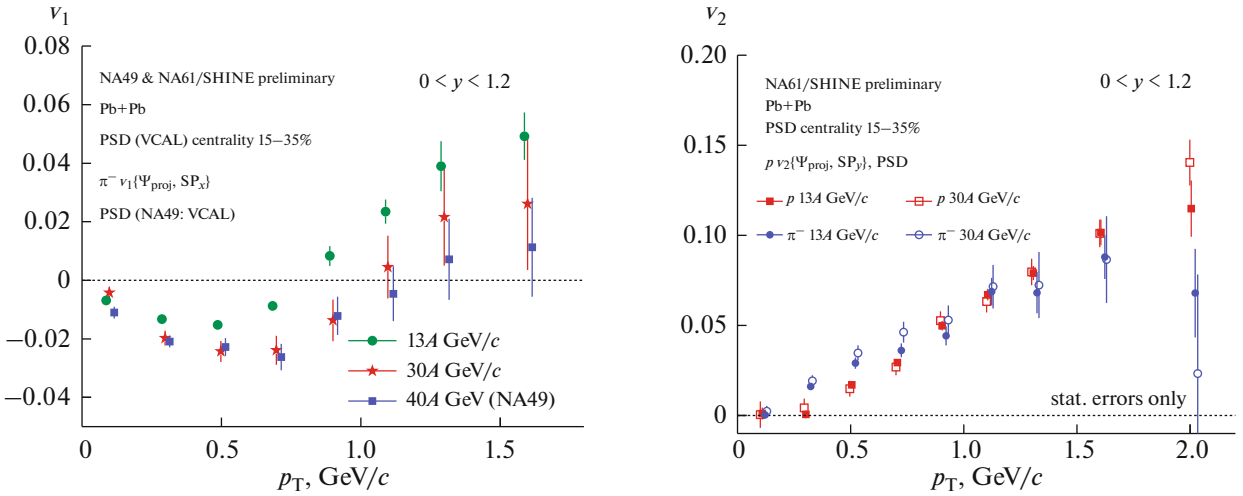

Fig. 3. Left: negatively charged pion directed flow $v_1(p_T)$ for beam momenta 13, 30A GeV/c [7] and kinetic energy of 40A GeV [6]. Right: elliptic flow $v_2(p_T)$ for protons and negatively charged pions at beam momenta 13 and 30A GeV/c.

Directed and elliptic flow for Pb–Pb collisions at at different energies are compared in Fig. 3. The NA49 results for 40A GeV were obtained using spectator plane estimated with Veto calorimeter (VCAL) which has a similar acceptance to the in NA61/SHINE PSD1 subevent. Directed flow (Fig. 3, left), in particular the p_T where v_1 changes its sign, shows strong collision energy dependence.

Elliptic flow $v_2(p_T)$ is different for negative pions and protons (Fig. 3, right) and shows weak energy dependence between 13 and 30 A GeV/c.

SUMMARY AND OUTLOOK

Directed and elliptic flow were measured relative to the spectator plane in Pb–Pb at 13, 30, and 40A GeV. Clear mass dependence is observed for v_1 and its slope dv_1/dy, and v_2. The directed flow shows strong energy dependence, with the slope of protons and negatively charged pions changing sign at different collision centralities.

It is planned to complete evaluation of the systematic uncertainties for 13, 30A GeV/c and 40A GeV, which involves study of p_T-y efficiency of tracking and sensitivity to purity of PID selection procedure. Analyses of Pb–Pb collisions at 150A GeV/c and other collision systems available in NA61/SHINE (Xe–La, Ar–Sc, etc.) are foreseeing in the nearest future.

FUNDING

This work was supported by the Ministry of Science and Education of the Russian Federation, grant no. 3.3380.2017/4.6, and by the National Research Nuclear University MEPhI in the framework of the Russian Academic Excellence Project (contract no. 02.a03.21.0005, 27.08.2013).

REFERENCES

1. S. A. Voloshin, A. M. Poskanzer, and R. Snellings, Landolt-Bornstein **23**, 293–333 (2010); arXiv: 0809.2949 [nucl-ex].
2. Y. Wu et al. [Star Collab.], Nucl. Phys. A **982**, 899–902 (2019); arXiv:1807.06738.
3. B. Kardan et al. [HADES Collab.], Nucl. Phys. A **967**, 812–815 (2017).
4. S. Afanasiev et al. [NA49 Collab.], Nucl. Instrum. Meth. A **430**, 210–244. (1999).
5. N. Abgrall et al. [NA61 Collab.], JINST **9**, P06005 (2014); arXiv:1401.4699 [physics.ins-det].
6. E. Kashirin et al. [NA49 Collab.], in *Proc. 13th Workshop on Particle Correlations and Femtoscopy (WPCF 2018)* (Krakow, 2018); arXiv:1810.07718.
7. V. Klochkov et al. [NA61/SHINE Collab.], Nucl. Phys. A **982**, 439–442 (2019); arXiv:1810.07579.
8. V. Klochkov et al. [CBM Collab.], *GSI Scientific Report **2015*** (2016), p. 8. https://doi.org/10.15120/GR-2016-1
9. A. M. Poskanzer and S. A. Voloshin, Phys. Rev. C **58**, 1671–1678 (1998); arXiv:nucl-ex/9805001.
10. TPC acceptance. https://edms.cern.ch/document/1549298/1.
11. PSD acceptance. https://edms.cern.ch/document/1867336/1.
12. I. Selyuzhenkov and S. Voloshin, Phys. Rev. C **77**, 034904 (2008); arXiv:0707.4672 [nucl-th].
13. V. Gonzalez, J. Onderwaater, and I. Selyuzhenkov, (2018), https://github.com/FlowCorrections/FlowVectorCorrections.
14. V. Gonzalez et al. [ALICE Collab.], *GSI Scientific Report 2015* (2016), p. 23; https://doi.org/10.15120/GR-2016-1